

# MECHANISM AND ANN MODELING OF SULFATE-INDUCED HEAVE IN NON-SWELLING SOIL IN AN ACIDIC ENVIRONMENT

## Abstract

Red earth (aluminosilicate) is mainly comprised of kaolinite mineral, which is of non-swelling in nature. The iron oxides present in the soil impart red colour to the earth, hence it is named red earth. In the case of natural 1:1 minerals, no significant volume changes are observed due to strong hydrogen bonding between their interlayers. Sulfate in an acidic environment can cause abnormal volume changes in natural red earth, owing to mineralogical alterations. Sulfuric acid solutions of varying concentrations are used to induce sulfate content in an acidic environment, which is a very common cause of acid sulfate soil contamination. When sulfuric acid starts interaction with red earth, the hydrated hydrogen ion starts attacking (due to smaller in size and/or ionic potential) on the red earth leading to a reduction in H-bonding between successive basic units of kaolinite and releasing the iron from iron oxides, results in the formation of new mineral rozenite (iron sulfate hydrate) in combination with sulfates. During this process, the heave reported in the red earth at nominal surcharge continued for a long period indicating that the formation of minerals was a rather slow process. The observed heave after considerable time lag, unlike the swell that occurs due to the adsorption of water by clay particles. The formation of new minerals is responsible for the observed non-hyperbolic nature of time swell relationships and the mineralogical and morphological changes are confirmed by scanning electron microscopy and energy dispersive analysis of X-ray studies. Besides, the sulfate-induced time-dependent swell percent in red earth in an acidic

## Author

**Guru Prasad. B**

Field Engineer

Water Resources Department

Government of Andhra Pradesh

Vijayawada, India.

bgurubpch@gmail.com

environment is studied by employing the Artificial Neural Network model with Levenberg–Marquardt (LM) algorithm. The network was programmed using MATLAB® code to process the information and predict the percent swell at any time, knowing the variable involved. Eight basic soil and fluid parameters were used as input feed to predict the percent swell to the proposed network. The study demonstrates that it is possible to develop a general ANN model that can predict time-dependent swell in sulfate-induced red earth with relatively high accuracy with observed data ( $R^2 = 0.9986$ ). The investigation results demonstrate reference to the engineering behaviour of acid sulfate soils, distributed worldwide under acidic environments.

**Keywords:** Acid Sulfate Contaminated Clays; Non-Swelling Soil; Rozenite Mineral; ANN Swell Modeling; Oedometer Consolidation; Morphology.

## I. BACKGROUND

The escalating pollution of the environment has been one of the greatest concerns of engineering in recent years owing to industrial advances in agriculture, expansion of chemical industries, and a general change in lifestyle all over the world have led to the release of a variety of pollutants into the environment, thus contaminating the atmosphere, water bodies, and many soil environments. Soil is a base for construction works, which requires profound study in modern-day construction activities, as soil contamination may cause unexpected issues for engineers. Realistically assessing the engineering properties of the contaminated soil is challenging as contaminated soil usage as a foundation material is pronounced in densely populated countries.

The main types of contaminants include inorganic acids, alkalis, sulfates, organic contaminants, toxic or phytotoxic metals, and combustible substances. In general, other than some natural processes, soils are increasingly being contaminated by anthropogenic sources such as leakages from waste containment facilities, accidental spills, and industrial operations. Apart from affecting biotic components of the ecosystem, these pollutants greatly affect the performance, behaviour, and stability of the soil system, thus causing severe damage to structures found on them. The hydraulic and/or chemical alterations which allow these polluting substances to move within soil pores lead to the physico-chemical decomposition process, chemical alterations, leaching, and ion exchange reactions. Such reactions could also result from natural processes such as weathering, but the effects caused by pollutants occur at faster rates. Soils are composed of clays, silts, and sands. Due to charged nature of the particles and their large specific surface, the engineering properties of expansive soils are greatly affected by pollutants.

Red soil is mainly comprised of kaolinite mineral, which is of non-swelling in nature. The high percentage of iron oxides present in the soil imparts red colour to the earth, hence it is named red earth. Expansive soils containing smectite minerals exhibit significant volume changes, that occur due to moisture variations which are negligible in soils containing predominantly minerals such as kaolinite. However, there are instances where unexpected swelling can occur in both swelling and non-swelling soils due to changes in the chemical environment. Most of these instances are associated with the presence of sulfate, particularly in the presence of lime. Several researchers have reported swelling and cracking in specimens of clay stabilized with lime and immersed in sulfate solutions [1], induced heave in lime-treated soil containing sulfate [2], Comprehensive studies on swell and shrinkage characteristics of lime-treated sulfate soil [3][4][5]. They have shown that the presence of sulfate increases the compressibility of lime-treated black cotton soil after curing for long periods. The presence of sulfate as gypsum induces deformation in lime-treated soils [6][7][8][9]. The effect of sulfate is due to the formation of ettringite and thaumasite in lime-treated soils containing sulfate. Thus, the presence of sulfate poses a problem with calcium-based stabilizers.

Moreover, the sulfate in the acidic environment of soil is an important aspect [10], as the distribution of acid sulfate soils worldwide is about 13 million hectares [11]. Due to soil acid sulfate interactions, roads, aircraft runways, railways, shallow underground service lines, retaining walls, and building foundations are severely affected. The common environmental condition that leads to the presence of sulfate in an acidic environment is the spillage of

sulfuric acid which is widely employed in many industries such as copper leaching, electroplating, lead-acid batteries, inorganic pigment production, metallurgy, petroleum refining, paper production, and industrial organic chemical production [12]. Owing to its widespread, improper usage and the difficulty in safe storage, sulfuric acid is often found as a contaminant in natural soils. Sometimes, due to volcanic sulfur dioxide photolysis, sulfuric acid percolates and contaminates the soil [13][14]. Batch experiments with kaolinite and bentonite clays suggested that acid rock drainage enhances the release of aluminum from these clays [15]. Recycled concrete was used as a reactive material in the permeable reactive barrier for the remediation of acidic groundwater in low-lying Acid Sulfate soil floodplains in Australia [16]. The mineralogical changes that occur due to the interaction of sulfate with minerals under an acidic environment have generated considerable interest because of developments on the environment on early Mars and their findings on sulfate seasonal behavior in an acid environment [16][17]. More recently, the experimental and computational study of sulfate mineral's structure and properties to understand its behavior at temperature conditions prevailing on the Martian surface and aid its identification in ongoing and future Rover missions [18][19]. While the effects of sulfate in the alkaline environment on the volume change behavior of soils are widely known, very little information is available on the same in an acidic environment.

Among the computing methods, artificial neural network imitates the computing models of the brain. How the inter-neuron connections are arranged and the nature of the connections determines the structure of a network. The strengths of the connections are adjusted or trained to achieve the desired overall behaviour of the network, which is governed by its learning algorithm. The availability of Neural Networks as detectors is based on their capability to incorporate a great quantity of information of several classes, their ability to generalize from noisy or incomplete information, and their robustness to ambiguities. Thus, the ANN approach is widely used in various civil engineering applications currently, little effort is made on modeling acid sulfate soils and their engineering behaviour [20]. Swelling in soils, which is a complex process, becomes even more complicated with the addition of sulfuric acid. Estimation of such chemically induced swelling will be useful to practicing engineers in general and for researchers in particular. Unfortunately, models to simulate chemically induced swelling in soils are hardly found in the literature. This is because the swelling behaviour of soil is highly non-linear, time-dependent, exhibit a huge amount of scatter, and is reliant on mineralogy. Consequently, the present study is principally aimed to understand the extent, nature, and cause of sulfuric acid-induced heave in natural red earth, in non-swelling kaolinite mineral and to demonstrates the artificial neural network model to envisage the percent swell at any time, knowing the variable involved.

## II. METHODOLOGY

- 1. Soil used:** Natural red soil that had been dug out from the campus of the Indian Institute of Science in Bangalore, India, was taken from a depth of about 1 m below the surface of the ground, dried in an oven at 105°C, and then used after being sieved using an Indian Standard 425 mm sieve. The soil is categorised as CL by the American Society for Testing Materials (ASTM), and X-ray diffraction investigations verified the existence of kaolinite mineral. Table 1 lists the geotechnical characteristics and elemental makeup of the numerous minerals found in soils, expressed as a percentage of oxides.

- 2. Preparation of Soil Specimen:** After being sieved through an Indian Standard 425 mm sieve, the dried soil samples were mixed with the optimum moisture content and kept in airtight polyethylene bags for about 7 days to allow the moisture to balance. The frequent range of sulfuric acid between 1 and 4 normal solutions is often thought to simulate sulfate contamination in an acidic environment. In order to achieve Proctor's maximum dry density ( $17.8 \text{ kN/m}^3$ ), Oedometer experiments were carried out on soil that had been combined to the ideal moisture content (18.3%) and statically compacted to a height of roughly 14 mm (Figure 1). The oedometer contained the consolidation cell with the ring attached. At a sitting pressure of 6.25 kPa, sulfuric acid solutions were poured over the samples. A dial gauge is utilized to track how the sample's height changes over time in the ring, and the swell percent is determined. To investigate the impact of sulfuric acid on the behavior of uncontaminated soil's volume change, the samples were submerged in solutions of 1 and 4 normal sulfuric acids. Additionally, a different set of tests were carried out on soil samples that had been saturated with the same fluid and compacted with 1 and 4 normal typical sulfuric acid solutions. These series illustrate how contaminated soil behaves in terms of volume change as a result of sulfuric acid contact. As a reference, tests were also carried out on soil samples that had been compacted and inundated with water.



**Figure 1:** Acid-Resistant Polypropylene Rings

- 3. Oedometer Tests:** As required by ASTM D2435, the one-dimensional consolidation tests were conducted. To complete the consolidation tests, the compacted samples in the consolidation rings were loaded and unloaded multiple times after being submerged in the necessary inundating fluid, allowing them to fully expand and reach equilibrium at seated load. To acquire swelling at a notional surcharge of 6.25 kPa until equilibrium was established, the changes in the specimen's height over time are recorded. The interaction of soil sulfate caused the swelling to be visible for a long time. With a load increment ratio of 1, loading up to 800 kPa and subsequent unloading was accomplished. Once the compacted sample is exposed to the inundating fluid in the oedometer cell, it will eventually
- swell at a minimal surcharge and
  - become compressible when the swell is complete.

The changes in the behaviour of soil due to interaction with sulfuric acid have been explained by mineralogical changes studied by X-ray diffraction studies, morphological changes investigated by Scanning Electron Microscopy (SEM), and elemental composition by Energy Dispersive X-ray technique (EDAX). In order to obtain average results and assess reproducibility, all laboratory tests were performed on triplicate specimens.

- 4. X-ray Diffraction Studies:** Following the consolidation test, soil samples were subjected to X-ray Diffraction examination utilizing a Philips diffractometer and radiation produced at 40 kV and 40 mA. Using silica gel as an adhesive, randomly oriented samples were prepared and placed on a glass slide before being exposed to Cu Ka radiation ( $\lambda = 10$  1.5148 Å) with a scanning speed of  $0.02^\circ$   $2\theta/s$ . For the purpose of diagnosing the sample, the recording's beginning and ending angles were kept at  $3^\circ$   $2\theta$  and  $70^\circ$   $2\theta$  respectively. Comparing each sample's diffraction pattern to benchmark patterns created by the Joint Committee of Powder Diffraction Data Service allowed researchers to make a qualitative assessment of the mineral types present in each sample [21].
- 5. Scanning Electron Microscope (SEM) and Energy Dispersive Analysis of X-ray (EDAX) Studies:** At a voltage range of 0.2--30 KV, a scanning electron microscope connected to an EDAX and SIRION was put to use to examine the morphology and elemental composition of soil samples. The oven-dried ( $105^\circ$  C) particle soil samples were placed on an aluminum stub that had double-sided carbon tape covering it. To stop a charging effect over the sample, a fine gold layer was vacuum-sputter-coated onto the sample's surface.
- 6. Soil and Fluid Parametric Tests:** The Geotechnical tests performed on acid sulfate soil include Atterberg's limits, compaction parameters, sediment volume, and volume change behaviour. Physico-chemical tests such as pH and electrical conductivity tests were performed to estimate the extent of interaction with sulfuric acid solutions. The size and shape of fine-grained mineral particles have strong influence on the specific surface area, thus SSA values were determined by water adsorption at 52% relative humidity.
- 7. Parameter and Data Selection for Neural Network Model:** The Levenberg–Marquardt (LM) algorithm is a prevalent algorithm to minimize nonlinear functions and was applied to develop the ANN model of swell percent estimation. The input layer in the artificial neural network model included eight significant parameters such as time (T), sulfuric acid normality (AC), liquid limit (LL), Plasticity Index (PI), Specific Surface area (SSA), Sediment Volume (SV), Hydrogen ion concentration (pH) and Electrical Conductivity (EC). Liquid limit and plasticity index were considered to represent common soil parameters in the swell modeling, which have been widely used to correlate with many soil properties. The concentration of sulfuric acid, pH, electrical conductivity of the soil, and fluid mixture were taken to represent the fluid parameters. It is well known that chemical reactions depend on pH conditions and electrical conductivity, apart from the duration of the interaction. The effect of soil-fluid interaction was considered in terms of the specific surface area and sediment volume (free swell index) of the soil with different concentrations of sulfuric acid solutions. Since the repetitive data slows down the training [22], the random selection method was used. A total of 1500 data sets were divided into

training group with 690 samples (46%) and testing group with 435 samples (29%) and the remaining 375 data sets (25%) were used for cross-validation of the network. The statistical parameters used in the present model are given in Table 4.

- 8. Model Development:** The Levenberg-Marquardt algorithm is employed to train the network using the LM algorithm in MATLAB® (platform V.7). The training and performance of the network are dependent on the criterion function to be minimized. The main steps in the design of the ANN technique are: (a) Analyzing performance variations for different numbers of inputs and hidden layers, and different numbers of nodes in these hidden layers; (b) Network training using the LM algorithm; and (c) Analysis of results.

### III. RESULTS AND DISCUSSION

- 1. Effect of Sulfuric Acid Solution on Volume Change Behavior Oo Red Earth Compacted with Water:** Figure 2 shows the percent swell of red earth compacted with water and inundated with water, 1 and 4 normal sulfuric acid solutions at nominal seating load. With water as an inundating fluid, only 0.35% of swell is observed when the sample reaches equilibrium in about 2 days. The low swell is due to mineralogy, and the inferior cation exchange capacity (Table 1). An abnormal swell of 24% is observed in the same soil when the inundating fluid is 1 normal sulfuric acid solution. This swell occurs for about 275 days. The swell further increases with 4 normal sulfuric acid as inundating fluid. A considerable swell of 55% is noticed when the sample reaches equilibrium in about 230 days. The induced swell by sulfuric acid can be explained as underneath:

Sulfuric acid dissociates into hydronium and sulfate ions in water. Initially, the hydronium ion, due to its smaller size and/or ionic potential, penetrates the crystal of the mineral structure leading to a reduction in H-bonding between successive basic units of kaolinite.

**Table 1: Geotechnical Properties and Chemical Composition of Soil**

Property	Value
Atterberg's limit (ASTM D2487)	
Liquid limit, LL (%)	38
Plastic limit, PL (%)	19
Plasticity index, PI (%)	19
Standard Proctor's (ASTM D2937)	
Maximum dry unit weight (kN/m <sup>3</sup> )	17.8
Optimum moisture content (%)	18.2
Specific gravity, G <sub>s</sub> (ASTM D854)	2.64
Grain size distribution (ASTM D422)	
Clay (%)	22
Silt (%)	44

Sand (%)	34
Soil classification (ASTM D2487)	CL
Primary mineral (JCPDS 1999)	Kaolinite
Cation exchange capacity, CEC (meq/100g) (ASTM D9081)	10.84
Sodium,Na (meq/100g)	0.82
Potassium,K (meq/100g)	0.38
Calcium,Ca (meq/100g)	6.86
Magnesium,Mg (meq/100g)	1.78
Chemical composition (%)	
SiO <sub>2</sub>	62.35
Al <sub>2</sub> O <sub>3</sub>	18.05
Fe <sub>2</sub> O <sub>3</sub>	2.61
MgO	1.67
CaO	5.91
K <sub>2</sub> O	0.42
Na <sub>2</sub> O	0.32
Other	0.21
Loss on ignition	8.41

Hydrogen ions can leach out iron present in the soil and can form a new mineral by association with dissociated anion,  $\text{SO}_4^{2-}$ . The new mineral formed is rozenite ( $\text{FeSO}_4 \cdot 4\text{H}_2\text{O}$ ) which is a form of iron sulfate hydrate. Further, from Figure 2, it can be observed that the delay in starting of swell process decreases with an increase in the concentration of inundating fluid. A lag period of 160 days was reported in soil inundated with 1 normal sulfuric acid, which reduces to 85 days with 4 normal sulfuric acid as inundating fluid.



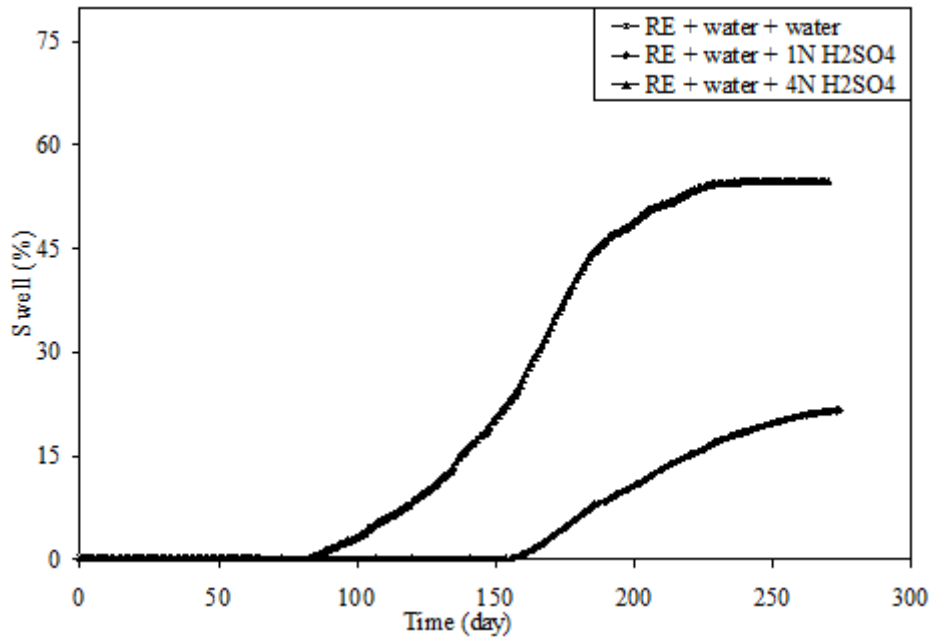


**Figure 2:** Comparison of Variation in Percent Swell with Time for Red Earth Remolded with Water and Inundated with Acid Solutions

The void ratio–pressure relationship for the soil samples remolded with water and inundated with water, 1 and 4 normal sulfuric acid is compared in Figure 3. It can be seen that compression, with an increase in the effective pressure, increases with the concentration of sulfuric acid.

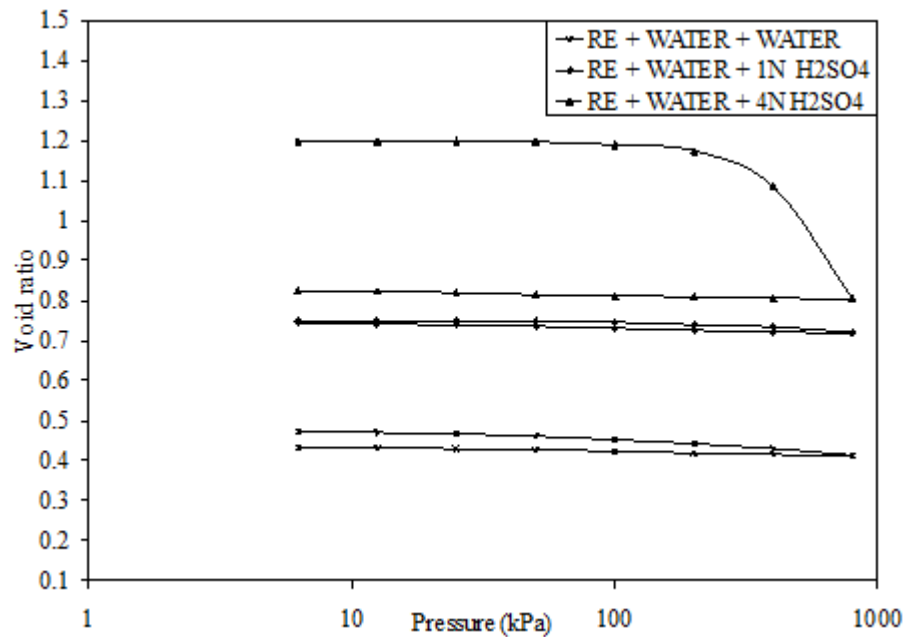


**Figure 3:** Void –Pressure Relationships of Red Earth Remolded with Water and Inundated with Acid Solutions

## 2. Effect of Sulfuric Acid Solutions on the Volume Change Behavior of Red Earth Compacted with Sulfuric Acid Solutions:

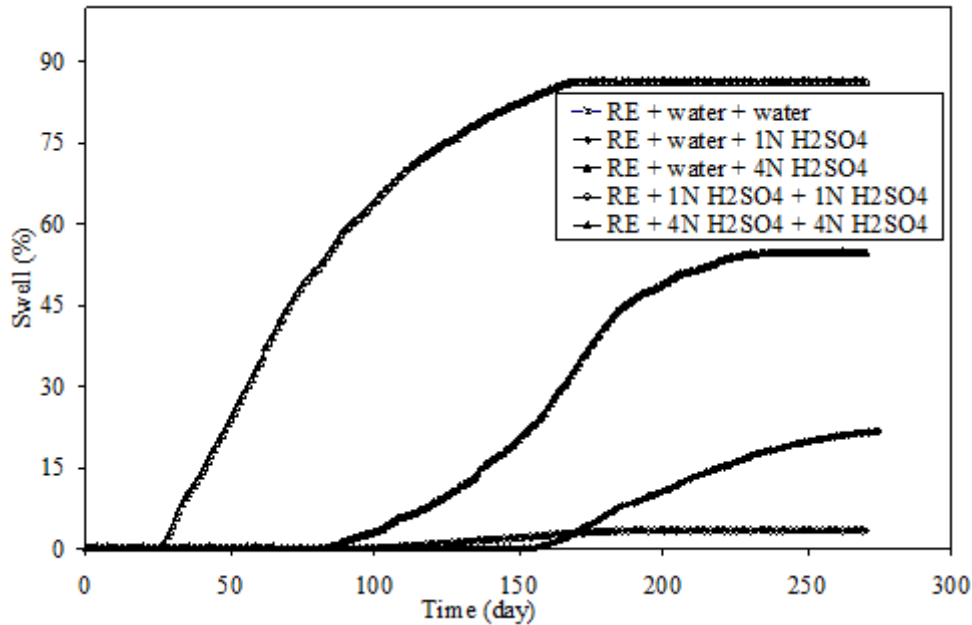


**Figure 4:** Comparison of Variation in Percent Swell with Time for Red Earth Remolded and Inundated with Acid Solutions

Figure 4 shows the percent swell of red earth compacted and inundated with 1 and 4 normal acid solutions. The sample compacted and inundated with 1 normal sulfuric acid shows swell of 3.5% reached in about 175 days, while the sample compacted and inundated with 4 normal sulfuric acid shows substantial swell of 85% in about the same period. Such an increase in swell percent is essentially due to mineralogical changes, as explained earlier. The lower swell in samples compacted with water than in samples compacted with acid might be due to the dilution of acid concentration due to water present in the samples compacted with water. Also, the starting of the swelling process occurs earlier in samples compacted with sulfuric acid than in samples compacted with water, though inundated with the same concentration of sulfuric acid. This might be due to the earlier initiation of mineralogical changes in samples compacted with acid solutions than compacted with water. The lower swell in the sample compacted and inundated with 1 normal acid solution might be due to less formation of rozenite than in the sample compacted with water and inundated with 1 normal acid solution (Figure 7).

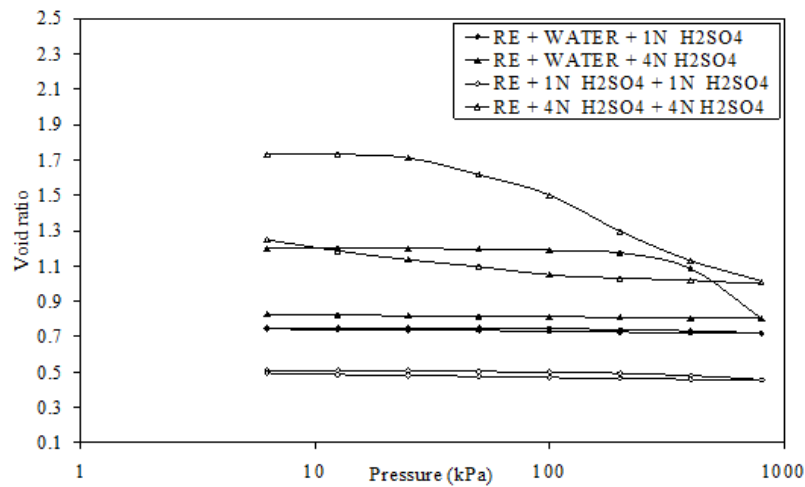


**Figure 5:** Void –Pressure Relationships of Red Earth Remolded and Inundated with Acid Solutions

The void ratio–pressure relationships of soil remolded and inundated with acid solutions are compared in Figure 5. The sample compacted and inundated with 4 normal sulfuric acid undergoes more compression than the sample compacted and inundated with 1 normal sulfuric acid. Further, it can be seen that the soil compacted and inundated with 1 normal sulfuric acid solution has undergone relatively less compression than soil compacted and inundated with 4 normal sulfuric acid, and is high compared with soils compacted with water. The soil compacted and inundated with 1 and 4 normal sulfuric acid would undergo higher compression than soil compacted with water but inundated with 1 and 4 normal sulfuric acid, respectively (Table 2). It can be seen that the soil compacted and inundated with 1 normal sulfuric acid 4 solutions has undergone relatively lower rebound than soil compacted and inundated with 4 normal sulfuric acid. The soil compacted and inundated with 1 and 4 normal sulfuric acid would undergo a higher rebound than soil compacted with water but inundated with 1 and 4 normal sulfuric acid, respectively (Table 2).

**Table 2:** Swell, Compression, and Rebound Values in Red Earth with Different Fluids

Re moulding fluid	Inundatng fluid	Maximm Swelling at 6.25 kPa, %	Compressio n, $\Delta e$	Total compressio n, $\Delta e/1+e_0$	Rebound, $\Delta e$
Water	Water	0.4	0.054	0.037	0.021
Water	1N Sulfuric acid	22.0	0.031	0.021	0.027
Water	4N Sulfuric acid	55.0	0.394	0.269	0.021
1N Sulfuric acid	1N Sulfuric acid	3.4	0.054	0.037	0.039
4N Sulfuric acid	4N Sulfuric acid	86.3	0.724	0.494	0.240

- 3. Nature of Time–Swell Relationships:** Apart from the magnitude of swelling, the time–swell relationship with remolding and inundating fluids was examined. It has been observed that the time–swell relationship of soil alone with water strictly follows hyperbolic pattern (Figure 6).

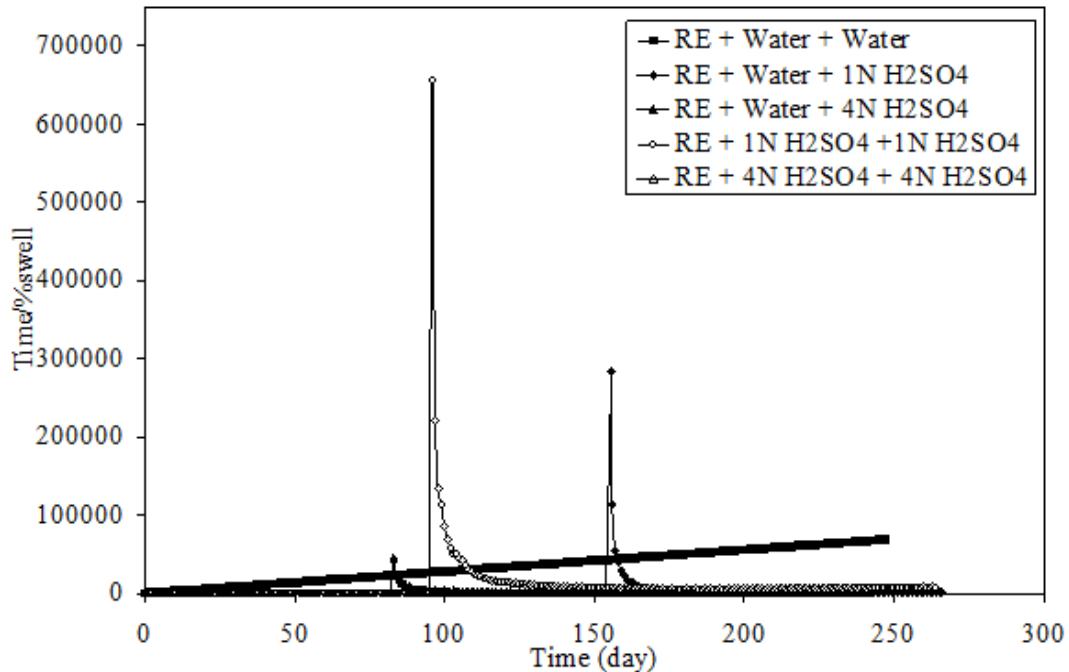


**Figure 6:** Time Vs. (Time/ %Swell) Relationships of Earth with Different Pore Fluids

However, the swell patterns observed for soil with 1 or 4 normal sulfuric acid solutions as remolding/inundating fluids do not show hyperbolic relationships (Figure 6). Further, the non-occurrence of the hyperbolic nature of curves shows the changes in mineralogy, which may be due to the very long period of interaction with an acid solution to complete the mineralogical changes. Thus, the starting of swell is delayed.

- 4. Mineralogical and Morphological Changes on Red Earth Samples:** K-Kaolinite; Q-Quartz; R-Rozenite; G-Gibbsite; C-Corundum

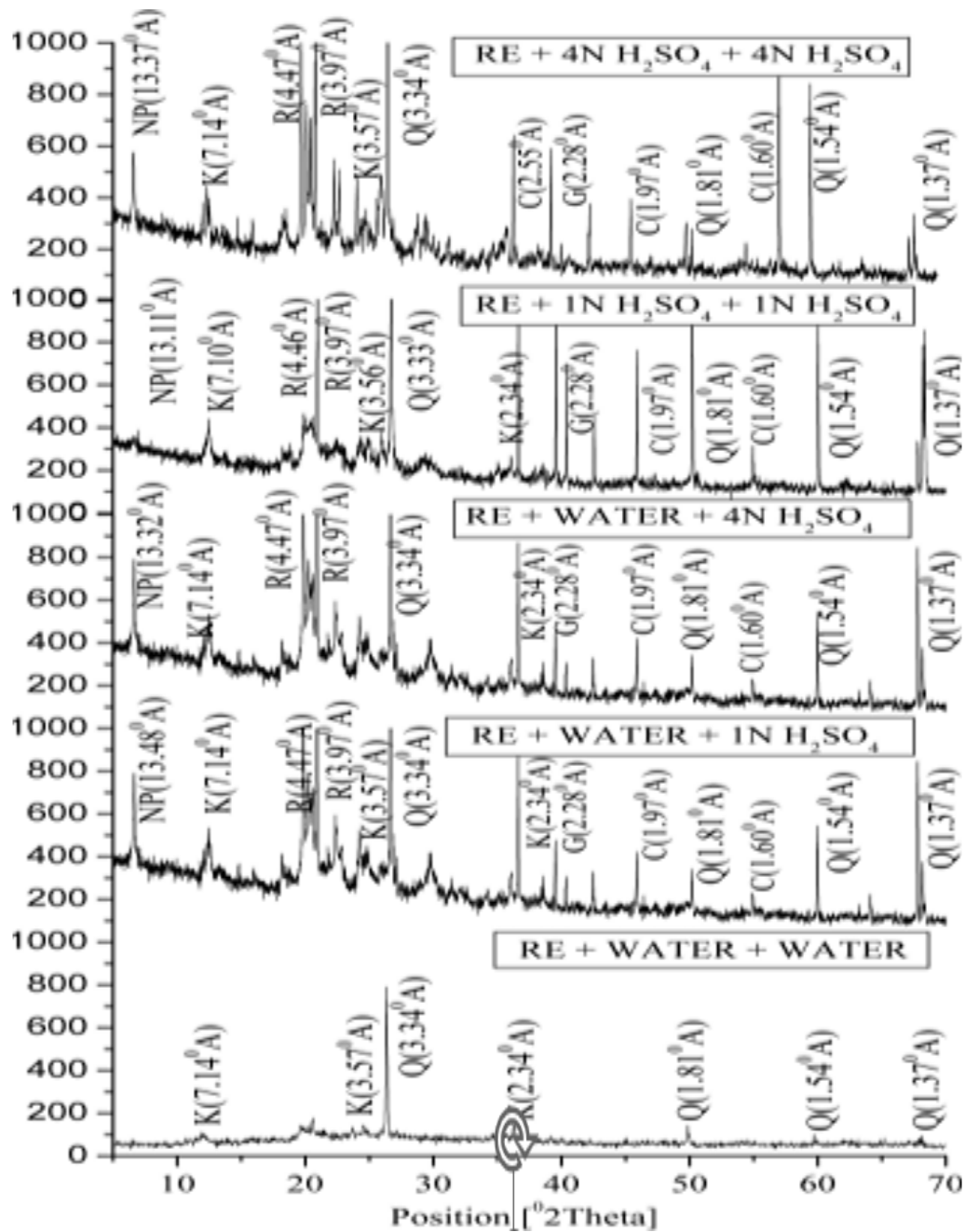


**Figure 7:** X-Ray Diffraction Patterns of Treated and Untreated Red Earth

The high percent of swell is slow and may be due to mineralogical changes occurring during consolidation. X-ray diffraction patterns of treated and untreated red earth are compared in Figure 7. Red earth has shown peaks at 7.14, 2.34, and 3.57 Å leading to the confirmation of kaolinite mineral. The soils inundated with acid solutions have shown rozenite mineral (peaks at 4.47, and 3.97 Å), which is an iron sulfate hydrate (Figure 7).

The Scanning Electron micrograph of red earth in Figure 8a exhibits a fairly compact and dense type of microstructure. This might be owing to the presence of iron-

bearing compounds has improved the dense nature of the red earth. Figures 8b--8e show the SEM micrograph of red earth inundated with sulfuric acid solutions taken after the completion of the consolidation test. The existence of flakes in shape and surface texture indicates the disintegration of moderately open type of microstructure. The open nature of the fabric has been attributed to the cation exchange process, which replaces inter-grain ions with a proton ( $H^+$ ). Exchangeable cations such as sodium, potassium, calcium, and magnesium are exchanged by hydrogen ions.

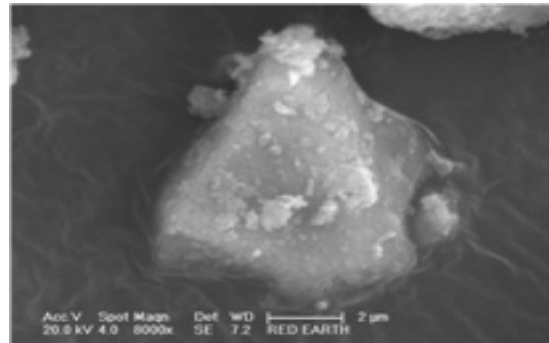


**Figure 8a:** Untreated Red Earth (Compact & Dense Unit)

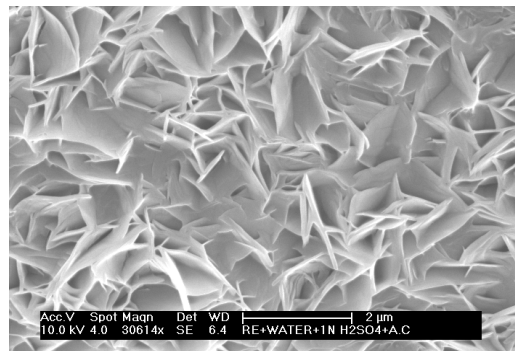


**Figure 8b:** Red Earth Remolded with Water and Inundated with 1N Sulfuric Acid Solution (Twinned Bladed Hexagonal Plates)

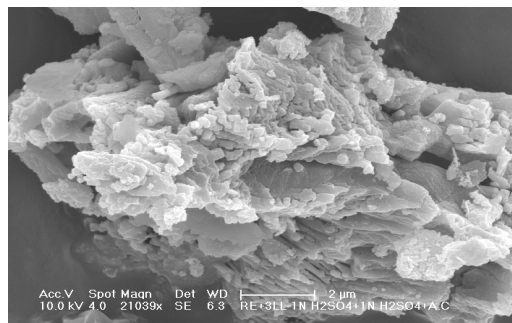


**Figure 8c:** Red Earth Remolded and Inundated with 1N Sulfuric Acid Solution (Plates And Laths Grouping)

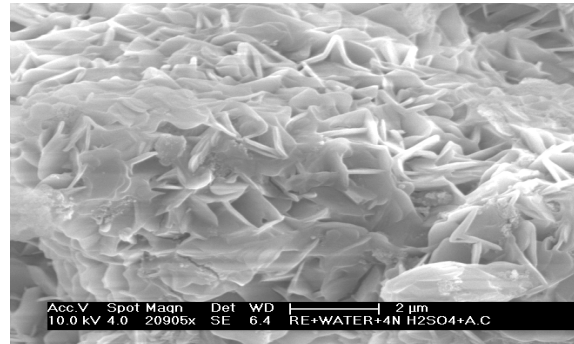


**Figure 8d:** Red Earth Remolded with Water and Inundated with 4N Sulfuric Acid Solution (Grouped Hexagonal Blades)

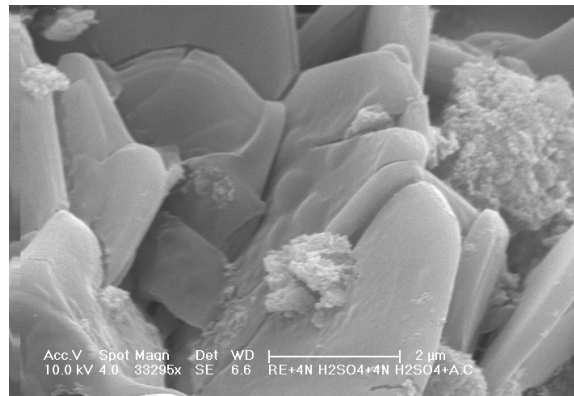


**Figure 8e:** Red Earth Remolded and Inundated with 4N Sulfuric Acid Solution (Larger Oriented Plated Units)

The energy dispersive analysis of X-ray (EDAX) elemental analysis, performed on samples, is compared in Table 3. The presence of iron ions is attributed to the presence of iron compounds in the red earth soil sample. Aluminum-to-silica ratios were evaluated for each sample using their weight percentages. They indicate the changes in chemical structure changes due to acid treatment. An increase in aluminum-to-silica ratios with an increase in the concentration of sulfuric acid is observed in all inundated samples. The sample compacted and inundated with 4 normal sulfuric acid undergoes a significant increase in aluminum-to-silica ratios compared to soil compacted with water and inundated with 4 normal sulfuric acid. In addition, the soil compacted and inundated with 1 normal sulfuric acid solution has undergone relatively less reduction in aluminum-to-silica ratios than soil compacted and inundated with 4 normal sulfuric acid. However, both these are higher Al-to-Si ratios compared with soils compacted with water.

**Table 3: Elemental Composition of Red Earth with Additives**

Soil and Pore Fluid	Weight (%)								
	Na	Mg	Al	Si	K	Ca	Fe	S	Al/Si
Red earth + water +water	47.11	0.12	0.06	3.00	48.13	0.23	0.06	1.29	0.02
Red earth + water +1N sulfuric acid	1.81	0.87	16.7	41.66	0.01	0.61	4.1	34.24	0.40
Red earth + water +4N sulfuric acid	0.79	0.65	17.78	34.65	0.11	0.12	0.08	45.82	0.51
Red earth + 1N sulfuric acid +1N sulfuric acid	3.02	.41	24.45	21.97	1.32	1.26	7.5	40.07	1.11
Red earth + 4N sulfuric acid +4N sulfuric acid	2.03	0.52	26.8	21.03	1.03	0.99	1.7	45.9	1.27

- 5. Prediction of Percent Swell using ANN Model in Red Earth in an Acid Sulfate Environment:** The stages of training include assembling the data, creating the network object, training the network, and simulating the ANN response to new inputs. An optimal neural network (8-8-1) was designed and presented in Figure 9.



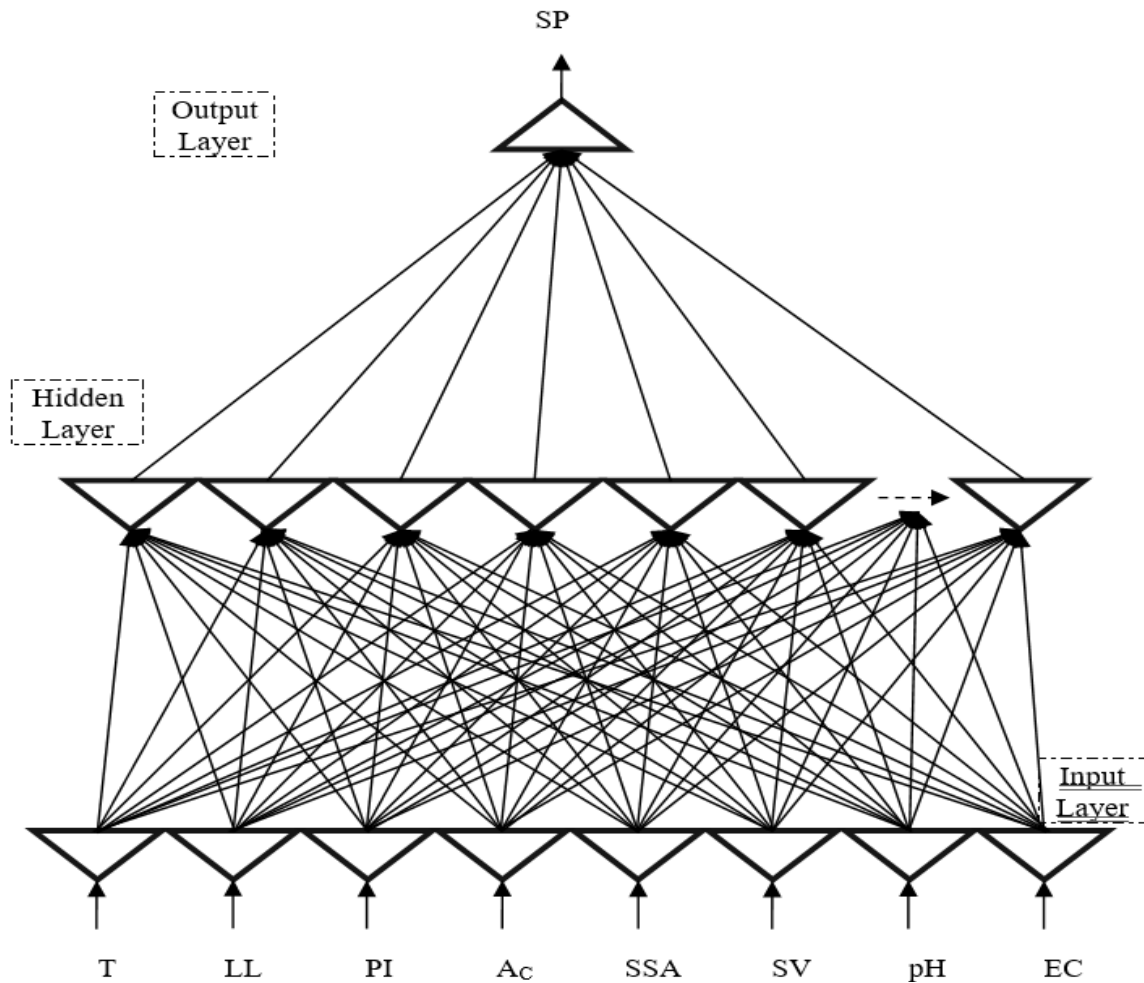


**Figure 9:** Typical Architecture of ANN Model

It was identified that the variation in training error with an increase in epoch was rapid up to 100 epochs, thereafter the reduction in error was significantly low, showing the proposed architecture could learn from the given inputs when it was trained for about 100 epochs. Figure 10 compares the behavior of the predicted swell using simple parameters with the experimental swell from the oedometer. The predicted and actual swell values for training and testing sets are shown  $R^2$  values as 0.9986 and 0.9925 with RMS errors as 0.5318 and 1.2323 respectively. The close correlation of the experimental and predicted percent swell of soil with 1 normal and 4 normal sulfuric acid inundated solutions indicates that the ANN model is capable of correlating the non-linear time series of swell to the multiple forcing given input signals.

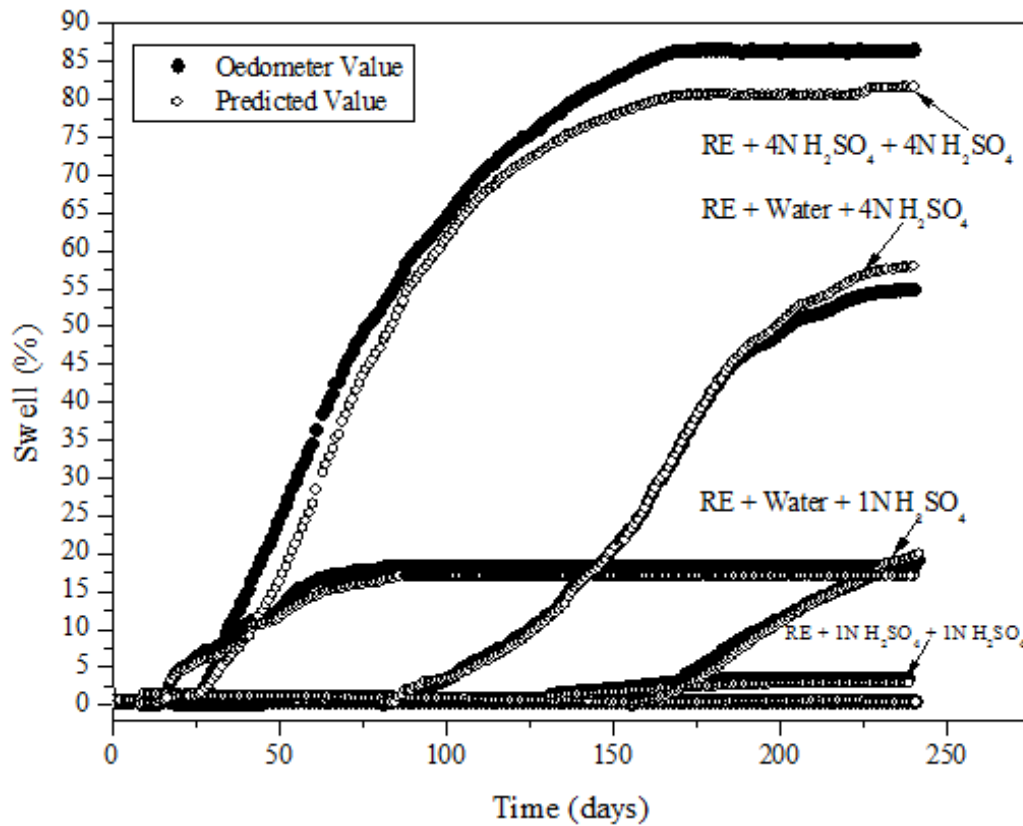


**Figure 10:** Behavior Comparison of the ANN Predicted Swell using Simple Parameters

- 6. Validation of Network:** Before the usage of a developed model, there is a need to establish the validity of the results it generates, hence separate data sets were assigned to this task. To check the strength of values comparison between the values of experimental swell and ANN predicted values shows the strong correlation coefficient ( $R^2 = 0.9982$ ) of the developed model leading to a conclusion that the network could provide almost perfect answers to the set of problems with which it was trained.
- 7. Proposed ANN Model Equation for the Swell Percent ( $S_p$ ) based on Trained Neural Network in an Acidic Environment:** The basic mathematical equation as per the ANN relating the input variables and the output can be written as

$$\text{Swell, } SP_{Pn} = f_{sig} \left\{ \sum_{k=1}^h W_k \times f_{sig} (b_{hk} + \sum_{i=1}^m w_{ik} X_i) \right\} \quad (1)$$

where  $SP_{Pn}$  is the normalized (in the range of -1 to 1)  $S_p$  value;  $w_k$  is the connection weight between  $k^{\text{th}}$  neuron of hidden layer and the single output neuron;  $b_{hk}$  is the bias at the  $k^{\text{th}}$  neuron of hidden layer;  $h$  is the number of neurons in the hidden layer;  $w_{ik}$  is the connection weight between  $i^{\text{th}}$  input variable and  $k^{\text{th}}$  neuron of hidden layer;  $X_i$  is the normalized input variable  $i^{\text{th}}$  in the range [-1, 1]. The distribution patterns of weights of the swell model are presented in Figure 11. Hence, the model equation for the output can be formulated based on the trained weights of the ANN model. In this case,

such a model equation for swell percent of acid sulfate soil was established using the values of the weights and biases as shown in Table 5 as per the following expressions.

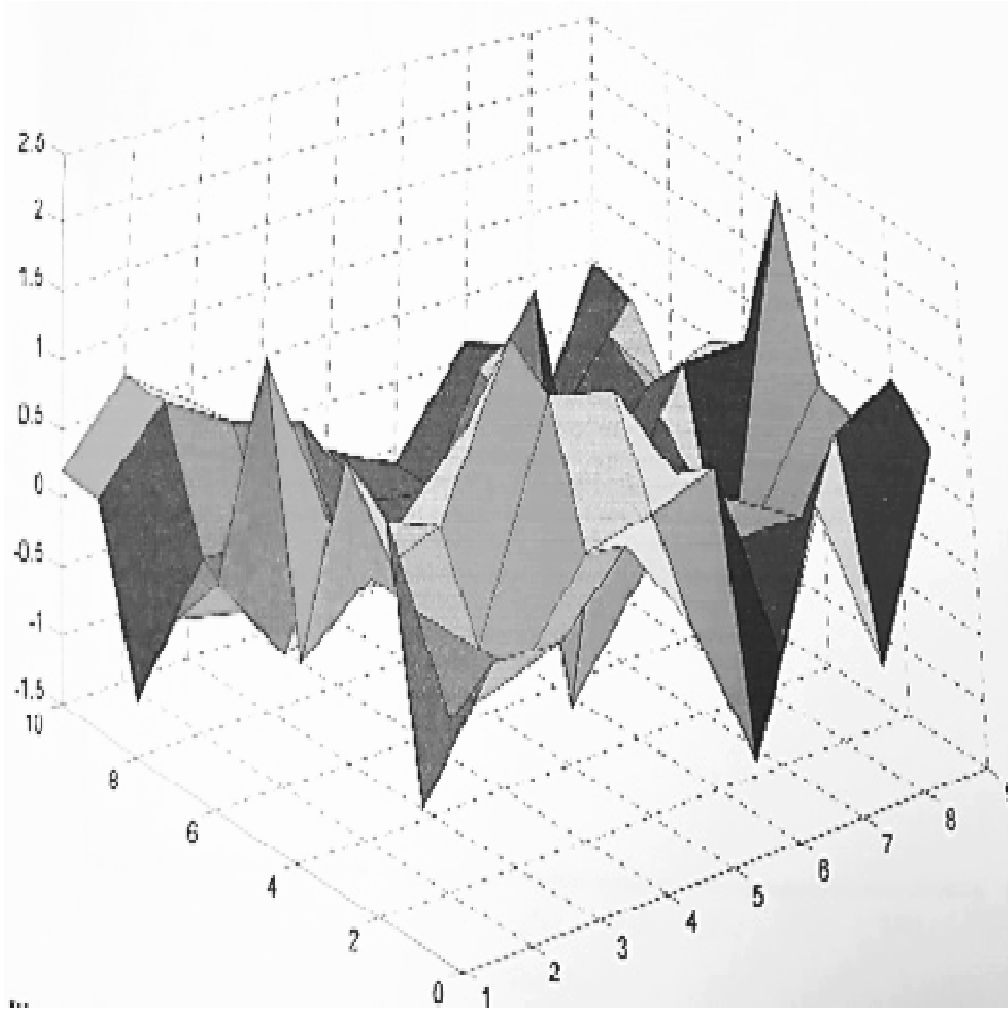


**Figure 11:** Distribution Patterns of Weights of Swell Model

**Table 4: Weights and Biases of the Artificial Neural Network Model in Acid Sulfate Red Earth**

Hidden Layer Neurons	Weights									
	Inputs								Output	Biase
	Time (T)	Liquid Limit(LL)	Plasticity Index (PI)	Sulfuric Acid Normality (A <sub>c</sub> )	Specific Surface Area (SSA)	Sediment Volume (SV)	pH	Electrical Conductivity (EC)	Swell (SP <sub>i</sub> )	b <sub>hki</sub>
i	C <sub>w1</sub>	C <sub>w2</sub>	C <sub>w3</sub>	C <sub>w4</sub>	C <sub>w5</sub>	C <sub>w6</sub>	C <sub>w7</sub>	C <sub>w8</sub>		
1	0.0979	-0.5641	-0.6042	1.0236	-0.3753	-0.9219	-0.7178	0.0635	-0.8458	0.9384
2	-0.3515	-0.3378	0.0491	-1.4742	0.1259	-1.2353	1.3589	-1.3054	0.4014	0.8321
3	-0.1809	0.1734	0.1805	1.2635	-0.3433	-0.6938	0.5210	0.2319	0.0546	1.4991
4	0.4334	-0.4133	0.4012	0.9085	0.2637	-0.6844	0.9693	0.1060	1.1125	2.4016
5	-1.4978	0.9179	0.6127	-1.8148	0.6922	0.8171	-1.5742	-0.5273	-0.4545	0.4447
6	-0.0848	0.9874	1.2427	-0.9992	-0.1494	-0.7596	1.0961	-0.9676	2.8451	1.7272
7	-0.7773	1.1518	0.9067	-1.4045	1.0722	0.7138	-0.8548	0.0879	-0.8382	0.6722
8	-1.4649	0.1562	0.1701	1.2570	-1.0254	-0.9586	0.8404	0.0193	0.0083	0.0301

$$P_i = \sum_{i=1}^N (SP_i) \frac{e^{G_i} - e^{-G_i}}{e^{G_i} + e^{-G_i}}$$

The generalised equation is as follows:

$$G_i = b_{hki} + C_{w1}(T) + C_{w2}(LL) + C_{w3}(PI) + C_{w4}(A_C) + C_{w5}(SSA) + C_{w6}(SV) + C_{w7}(pH) + C_{w8}(EC) \quad (2)$$

$$G_1 = 0.9384 + 0.0979(T) - 0.5641(LL) - 0.6042(PI) + 1.0236(A_C) - 0.3753(SSA) - 0.9219(SV) - 0.7178(pH) + 0.0635(EC) \quad (2a)$$

$$G_2 = 0.8321 - 0.3515(T) - 0.3378(LL) + 0.0491(PI) - 1.4742(A_C) + 0.1259(SSA) - 1.2353(SV) + 1.3589(pH) - 1.3054(EC) \quad (2b)$$

$$G_3 = 1.4991 - 0.1809(T) + 0.1734(LL) + 0.1805(PI) + 1.2635(A_C) - 0.3433(SSA) - 0.6938(SV) + 0.5210(pH) + 0.2319(EC) \quad (2c)$$

$$G_4 = 2.4016 + 0.4334(T) - 0.4133(LL) + 0.4012(PI) + 0.9085(A_C) + 0.2637(SSA) - 0.6844(SV) + 0.9693(pH) + 0.1060(EC) \quad (2d)$$

$$G_5 = 0.4447 - 1.4978(T) + 0.9179(LL) + 0.6127(PI) - 1.8148(A_C) + 0.6922(SSA) + 0.8171(SV) - 1.5742(pH) - 0.5273(EC) \quad (2e)$$

$$G_6 = 1.7272 - 0.0848(T) + 0.9874(LL) + 1.2427(PI) - 0.9992(A_C) - 0.1494(SSA) - 0.7596(SV) + 1.0961(pH) - 0.9676(EC) \quad (2f)$$

$$G_7 = 0.6722 - 0.7773(T) + 1.1518(LL) + 0.9067(PI) - 1.4045(A_C) + 1.0722(SSA) + 0.7138(SV) - 0.8548(pH) + 0.0879(EC) \quad (2g)$$

$$G_8 = 0.0301 - 1.4649(T) + 0.1562(LL) + 0.1701(PI) + 1.2570(A_C) - 1.0254(SSA) - 0.9586(SV) + 0.8404(pH) + 0.0193(EC) \quad (2h)$$

The  $SP_{Pn}$  value as obtained from Eq. (2) is in the range [-1, 1] and this needs to be denormalized as

$$SP_P = S_{Pn \text{ model}} (S_{P \text{ max}} - S_{P \text{ min}}) + S_{P \text{ min}} \quad (3)$$

Where,

$SP_P$  = Predicted model swell percent;  $SP_{Pn \text{ model}}$  = The model output;

$S_{P \text{ max}}$  = The maximum swell percent; and  $S_{P \text{ min}}$  = The minimum swell percent

The swell percent in acid sulfate soil,  $S_P = \frac{e^{pi} - e^{-pi}}{e^{pi} + e^{-pi}}$

- 8. Sensitivity Analysis:** On the trained percent swell, a step-by-step sensitivity test was performed by gradually changing each input neuron at a fixed rate. In the investigation, different constant rates (-5, 5, 10, and 20%) were chosen. The percentage change in the output due to a change in the input neuron was detected for each input neuron. The following approach is applied to calculate each input neuron's sensitivity:

$$\text{Sensitivity} = \frac{1}{N} \sum_{j=1}^N \left( \frac{\% \text{change in output}}{\% \text{change in input}} \right)_j \times 100 \quad (4)$$

where,

N = number of data sets used in the study

Figure 12 shows how sensitive the percent swell was, at each of the selected input parameters and how they would affect the changes. Almost all the selected parameters showed the significant contribution to the percent swell in acid sulfate soil.

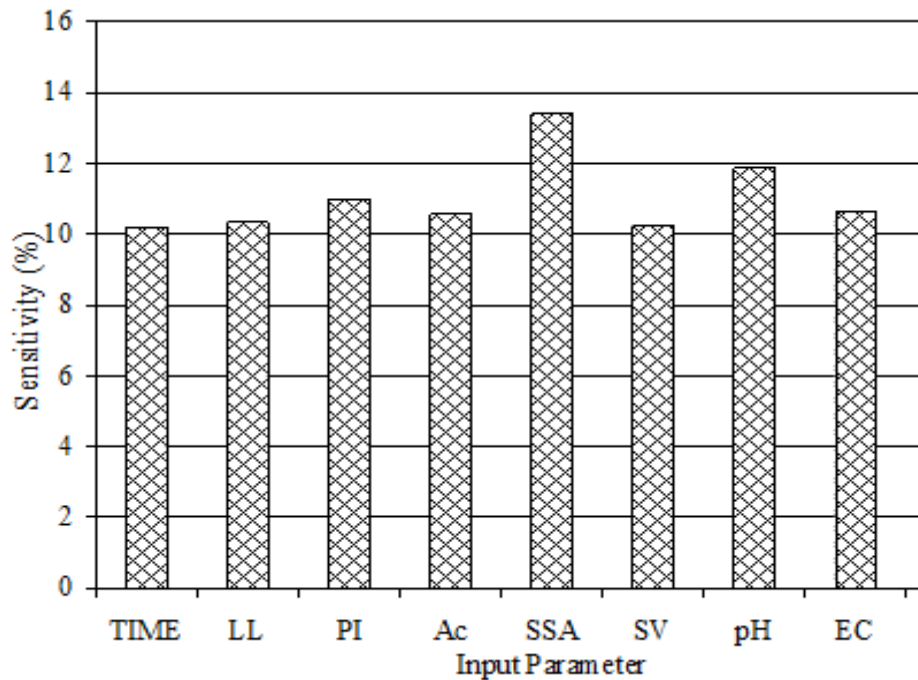


**Figure 12:** Typical Variation of Input on the Output Using Sensitivity Analysis

#### IV. CONCLUSIONS

The changes in the behaviour of red earth during contamination and continued contamination were studied using oedometer swelling tests with a prolonged time to bring the effect of soil acid sulfate interaction. Understanding and computing the soft modeling of the engineering behaviour of acid-contaminated soil is a challenging task with the influence of mineralogy. Based on the data presented the following conclusions are drawn:

1. The presence of sulfate in an acidic environment will induce swell in non-swelling kaolinitic soils. Sulfate content plays a significant role in the magnitude of swell.

2. Breakage of hydrogen bonding between its layers and mineralogical changes, leading to the formation of new mineral rozenite, are responsible for induced heave.
3. The swell in the presence of sulfate is initiated after considerable time due to a fair degree of mineralogical changes. Delay decreases with an increase in the concentration of sulfate. Thus, the induced swell–time relationships do not follow conventional hyperbolic nature.
4. The acid sulfate interacted soil in oedometer swell tests showed the existence of flakes in shapes and the cauliflower-like surface texture in scanning electron microscopy indicated the disintegration of a moderately open type of microstructure, conforms to the induced swell in red earth. However, the natural red earth exhibited a fairly compact and dense type of microstructure.
5. The swell percent obtained for sulfuric acid contaminated red earth by ANN technique with basic properties as input feed showed a good correlation with an experimental swell leading to a conclusion that ANN could be applied even to complex problems, using Levenberg-Marquardt algorithm to obtain a quick preliminary assessment.

## REFERENCES

- [1] P.T.Sherwood, "Effect of sulfate on cement and lime treated soils," Highway Research Board Bull. No. 353, pp.98-107, 1962.
- [2] D. Hunter, "Lime induced heave in sulfate bearing clay soils," Journal of Geotechnical Engineering, ASCE, Volume 114, Issue 2, pp.150-167, 1988.
- [3] P.V.Sivapullaiah, A.Sridharan, and H.N.Ramesh, "Effect of sulfate on the volume change behavior of lime treated kaolinitic soil," Proc. Second Int. Seminar on Soil Mech. and Found. Eng., Iran, pp.140-159, 1993.
- [4] A.Sridharan, P.V.Sivapullaiah, and H.N.Ramesh, "Consolidation behavior of lime treated sulfatic soils," International Symposium on compression and consolidation of clayey soils, Hiroshima, Japan, pp.183-188, 1995.
- [5] A.Sridharan, P.V. Sivapullaiah, and H.N. Ramesh, "Consolidation behavior of lime treated red earth with sulfate content," Int. Natl. Conference on Ground Improvement Techniques, Macau, 6-8 May, pp.531-539, 1997.
- [6] A. J. Puppala, C.Dunker, S.Hanchanloet, and K.Ghanma, "Swell and shrinkage characteristics of lime treated sulfate soil," Texas ASCE, Spring Meeting Proceedings, Texas, April, 1998.
- [7] A. J.Puppala, S.Hanchanloet, M.Jadeja, and B.Burkart, "Evaluation of sulfate induced heave by mineralogical and swell tests," XI Pan- American Conference on Soil Me-chanics and Geotechnical Engineering, Foz do Iguacu, Brazil, August, 1999.
- [8] P. B. V. S.Kota, D.Hazlett, and L.Perrin, "Sulfate-bearing soils: Problems with calcium based stabilizers," Transportation Research Record, 1546, Transportation Research Board, Washington, DC, pp.83-91, 1996.
- [9] B.Burkart, C. G.Goss, and P. J.Kern, "The role of gypsum in production of sulfate-induced deformation of lime-stabilized soils," Environmental & Engineering, Geoscience, 5(2), pp.173-187, 1999.
- [10] J.Sammut, and R.Lines-Kelly, "An introduction to acid sulfate soils," ASSMAC, Dept., Environment, Sport and Territories, Australian Seafood Industry Council, 1996.
- [11] R. Brinkman, " Social and economic aspects of the reclamation of acid sulfate soil areas," The International Rice Research Institute, Philippines, pp.21-51, 1982.
- [12] P.V. Sivapullaiah, M.M. Allam, "Effect of Sulfuric Acid on Swelling Behavior of an Expansive Soil," Soil and sediment contamination, pp.121-135, 2009.
- [13] R. K. Rowe, "Movement of pollutants through clayey soil," Keynote Lecture, ACADS Seminar on Modelling of Contaminant Migration, Melbourne, Australia, April, pp.1-34, 1991.
- [14] B.Indraratna, J. Sullivan, and A. Nethery, "Effect of groundwater table on formation of acid sulphate soils," Minewater and the Environment, 14(1), pp.71-83, 1995.
- [15] O.Vazquez, X. Pu, J.D. Monnell, and R.D. Neufeld, "Release of Aluminium from clays in an acid rock drainage environment," Mine water and the environment. June, 2010.



- [16] G.Regmi, B.Indraratna,L.D.Nghiem,A.Golab, and B. Guru Prasad, "Treatment of Acidic Groundwater in Acid Sulfate Soil Terrain Using Recycled Concrete: Column Experiments," *Journal of Environmental Engineering*, pp.433-443,2010.
- [17] S. Paramanick, V.J. Rajesh, M.N. Praveen and K.S. Sajinkumar "Spectral and chemical characterization of Copiapite and Rozenite from Padinjarathara in Wayanad, southern India: Possible implications for Mars Exploration," *Chemical Geology*, 575(1):2020.
- [18] T.Fornaro, A. Steele and J.R. Brucato, "Catalytic/Protective Properties of Martian Minerals and Implications for Possible Origin of Life on Mars," *Life*, pp.1-41,2018.
- [19] J.M. Meusbarger, K.A.Hudson-Edwards, C.C.Tang, E.T.Connolly, R.A.Crane, A.D.Fortes "Low-temperature crystallography and vibrational properties of rozenite (FeSO<sub>4</sub>·4H<sub>2</sub>O), a candidate mineral component of the polyhydrated sulfate deposits on Mars," *American Mineralogist*, pp. 1080-1091,2023.
- [20] B. Guru Prasad,B.Indraratna,L.D.Nghiem and G.Regmi, "A neural network approach to predict the performance of recycled concrete used in permeable reactive barriers for the treatment of acidic groundwater," *Quarterly Journal of Engineering Geology and Hydrogeology*,pp.199-209,2011.
- [21] JCPDS, "Joint Committee for Powder Diffraction Studies," International Centre for Diffraction Data, The Powder Diffraction File, 1999.
- [22] ASCE Task Committee, "Artificial Neural Networks in Hydrology. I: Preliminary Concepts", *Journal of Hydrologic Engineering*, pp.124-144,2000.